

- near saturated stream of water vapor in argon. CFs formed by condensation of water as the stage was cooled to $\sim 0^\circ\text{C}$.
- To form the patterned SAMs of alkanethiolates on a gold substrate, a micropipen was used first to write lines of a hydrophobic SAM from neat hexadecanethiol [$\text{HS}(\text{CH}_2)_{15}\text{CH}_3$], and then a micropipette was used to form a hydrophilic SAM from mercaptohexadecanoic acid [$\text{HS}(\text{CH}_2)_{15}\text{CO}_2\text{H}$]; see A. Kumar, H. A. Biebuyck, N. L. Abbott, G. M. Whitesides, *J. Am. Chem. Soc.*, in press. The SAM derived from $\text{HS}(\text{CH}_2)_{15}\text{CH}_3$ was written in air. To write the hydrophilic line, a micropipette was loaded with a concentrated solution of $\text{HS}(\text{CH}_2)_{15}\text{CO}_2\text{H}$ in hexadecane. The tip of the micropipette and the gold surface were placed under water. The water prevented spreading and trailing of the thiol solution during writing. During writing, the tips of the pen and micropipette did not touch the surface of the gold; only liquid containing the alkanethiol contacted the gold. There was therefore no mechanical marking of the gold surface. After formation of the desired patterns, the gold was exposed to a 1 mM solution of $[\text{S}(\text{CH}_2)_{16}\text{CN}]_2$ for 1 min. The disulfide $[\text{S}(\text{CH}_2)_{16}\text{CN}]_2$, rather than the corresponding thiol, was used to complete the SAM of alkanethiolates because the rate of exchange of the preformed, alkanethiolate SAMs (lines in Fig. 1) is slower with disulfide than with thiol (H. A. Biebuyck and G. M. Whitesides, unpublished results).
 - The line was obtained by writing of $\text{HS}(\text{CD}_2)_{15}\text{CD}_3$ with a micropipen in air. A 1 mM $\text{HS}(\text{CH}_2)_{15}\text{CO}_2\text{H}$ solution in ethanol was reactively spread on either side of the hydrophobic line and allowed to react for 1 min to derivatize the remainder of the gold surface.
 - Typical SIMS analysis conditions were as follows. A primary ion beam of 16 keV Ga^+ ions (50 pA) was used. The maps obtained are a 256 pixel by 256 pixel image with a dwell time of 200 μs per pixel. We believe the peak at a mass-to-charge ratio $m/z = 50$ to be primarily due to C_3D_7^+ ; that at $m/z = 55$ is attributable to $\text{C}_3\text{H}_5\text{O}^+$ and C_4H_7^+ . For further details see C. D. Frisbie, J. R. Martin, R. R. Duff, M. S. Wrighton, *J. Am. Chem. Soc.* 114, 7142 (1992).
 - G. P. López, H. A. Biebuyck, G. M. Whitesides, unpublished results; E. W. Wollman, C. D. Frisbie, M. S. Wrighton, unpublished results.
 - Pyrex glass wafers (Mooney Precision Glass, Huntington, WV) were cleaned in piranha solution [see (5)], rinsed with deionized water, and dehydrated under N_2 at 200°C for 8 hours. A 1- μm layer of positive photoresist (KTI 820, 20 centistokes, Union Carbide) was spin coated onto the glass wafers. The coated wafers were baked at 90°C for 30 min and then exposed to ultraviolet light in an infrared aligner (Carl Suss, Munich, Germany) through a chrome mask containing the desired pattern. We removed the exposed photoresist by treating the photoresist with KTI-934 (1:1) developer (Union Carbide). The remaining photoresist was used to restrict the deposition of vaporized (tridecafluoro-1,1,2,2-tetrahydrooctyl)-1-trichlorosilane [$\text{Cl}_3\text{Si}(\text{CH}_2)_2(\text{CF}_2)_5\text{CF}_3$] to certain regions of the surface of the glass. Photopatterned glass wafers were placed in a vacuum desiccator (in a dry box) together with an open vial containing 30 μl of $\text{Cl}_3\text{Si}(\text{CH}_2)_2(\text{CF}_2)_5\text{CF}_3$ for 20 min. The vial and the remaining liquid were then removed from the desiccator, which was evacuated with continuous pumping for 1 hour. The wafers were then removed from the desiccator, and the photoresist was lifted off by sonication in ethanol. After drying, the newly exposed glass surfaces were derivatized (as above) by exposure to 10-undecenyl-1-trichlorosilane [$\text{Cl}_3\text{Si}(\text{CH}_2)_9\text{CH}=\text{CH}_2$] vapors. This procedure resulted in a patterned surface of fluorinated and vinyl-terminated monolayers. We then selectively rendered the vinyl-terminated monolayers hydrophilic by placing the wafers in an aqueous oxidant solution (1.0 mM KMnO_4 ; 40 mM NaIO_4 ; 4 mM K_2CO_3 ; pH 7.5) for 15 min. The wafer was removed from this solution and rinsed in 10 ml of each of 1 M

- NaHSO_3 , water, 0.1 N HCl, and ethanol [see (7)].
- L. Vroman, *Thromb. Diath. Haemorrh.* 10, 455 (1963); H. Elwing, *FEBS Lett.* 111, 365 (1980).
- P. A. Laibinis, R. L. Graham, H. A. Biebuyck, G. M. Whitesides, *Science* 254, 981 (1991).
- M. J. Tarlov, *Langmuir* 8, 80 (1992).
- C. Bubeck, *Thin Solid Films* 178, 483 (1989).
- H. A. Biebuyck and G. M. Whitesides, unpublished results.
- We thank R. Singhvi for providing the photopatterned poly(methyl methacrylate)-glass samples for silanization. This research was supported in

part by the Office of Naval Research and the Defense Advanced Research Projects Agency. We obtained SIMS ion maps using instrument facilities purchased under the Defense Advanced Research Projects Agency-University Research Initiative program. G.P.L. thanks the Ford Foundation for a postdoctoral fellowship and the National Institutes of Health for supplementary funds provided under the initiative to increase the participation of underrepresented minorities in research.

9 November 1992; accepted 17 February 1993

Condensed-Matter Energetics from Diatomic Molecular Spectra

In Ho Kim, Raymond Jeanloz,* Kyu Soo Jhung

Analyses of molecular spectra and compression data from crystals show that a single function successfully describes the dependence on interatomic separation of both the potential energy of diatomic molecules and the cohesive binding energy of condensed matter. The empirical finding that one function describes interatomic energies for such diverse forms of matter and over a wide range of conditions can be used to extend condensed-matter equations of state but warrants further theoretical study.

Prediction of the energetics of many-body systems from a detailed model of two-body interactions among the constituent particles has long been a matter of interest. Thus, considerable effort has gone into the derivation of reliable expressions for the potential-energy functions of two-atom systems (1, 2), and substantial progress has been made toward the discovery of a universal description of these diatomic potentials (3–8). Ideally, such a universal description reduces to a single potential-energy function that is valid for all diatomic systems. Similarly, universal correlations have been uncovered in recent work on the energetics of many-atom systems. For example, one equation of state appears to describe interparticle forces ranging from adhesion at large separations to nuclear compression at short ranges (5, 9). Here we develop in more detail, and using a different approach, a surprisingly reliable description of binding energy that spans the range from diatomic molecules to condensed matter (10).

The binding energy of a diatomic molecule can be expressed as a modified Dunham expansion of the reduced energy $f = E(R)/E_e$, which has the form

$$f(z_1) = z_1^2 \left(1 + \sum_{n=1}^{\infty} \beta_n z_1^n \right) - 1 \quad (1)$$

in terms of the linear scaled distance used by many investigators (5–11)

$$z_1 = \sqrt{\Delta} (R/R_e - 1) \quad (2)$$

Here R_e and E_e are the equilibrium values of the interparticle distance R and potential energy $E(R)$ of the molecule. The β_n are related to the Dunham coefficients, a_n , by the relation $\beta_n = a_n/\Delta^{n/2}$, where Δ is the Sutherland parameter, a material-dependent scale factor corresponding to the equilibrium force constant of a harmonic oscillator (11, 12). If all β_n equal zero, the reduced potential f is that of a harmonic oscillator. Alternatively, if we assign an equal amount of anharmonicity to all diatomic molecules, then each β_n is independent of the molecule involved (13).

Diatomic molecules exhibit a wide range of anharmonicity, however, and linear scaling of interatomic distances as given by Eq. 2 is inadequate because it implies β_1 and β_2 are constant for all systems (Fig. 1A). Instead, a more flexible nonlinear scaling, including molecule-dependent excess parameters, seems to be required. This is facilitated by the observation that the spectroscopically determined anharmonicity parameters β_1 and β_2 are correlated (Fig. 1A'). The strong correlation is not limited to two dimensions but still holds in multidimensional β -space, at least up to four β -dimensions (14). Therefore, we can regard this correlation as an expression that can generate β_{n+1} from β_n , a recursion relation for

I. H. Kim, Department of Geology and Geophysics, University of California, Berkeley, CA 94720, and Agency for Defense Development, Yuseong Post Office Box 35, Taejeon 305-600, South Korea.
R. Jeanloz, Department of Geology and Geophysics, University of California, Berkeley, CA 94720.
K. S. Jhung, Agency for Defense Development, Yuseong Post Office Box 35, Taejeon 305-600, South Korea.

*To whom correspondence should be addressed.

the binding-energy curve, at least in an approximate sense. Because most of the data are closely distributed around a single curve in β -space (Fig. 1A), we take the curve to define an exact recursion relation among the β_n , which is significant because one can always determine a single expression for the potential energy if such a recursion relation is known (8).

In our approach, we replace the linear distance z_1 in the n th term of the summation (Eq. 1) with a nonlinear distance variable z_n given by an n -degree polynomial in z_1 having coefficients that include all the material dependencies. If the form of expansion given in Eq. 1 is retained, the first few nonlinear scaled distances are (8)

$$z_2 = z_1 + \frac{1}{2} (\beta_1 - h_1) z_1^2 \quad (3)$$

$$z_3 = z_2 + \frac{1}{2} \left(\beta_2 - \frac{1}{4} \beta_1^2 - h_1 \beta_1 + \frac{5}{4} h_1^2 - h_2 \right) z_1^3 \quad (4)$$

Because the differences between individual data points and the β -curve are absorbed into the polynomial coefficients, the remaining material-independent part (the β -curve) defines a universal expression for the potential energy and involves only a small number of parameters.

We can determine the $\{h\}$ set by minimizing the square of each term in parentheses in Eqs. 3 and 4 successively, so that the z_n have a maximum convergence. For the 339 molecular data in Fig. 1A, we obtain $h_1 = -1.028 \pm 0.011$ and $h_2 = 0.670 \pm 0.005$ (15), and the conditions that make the coefficients in Eqs. 3 and 4 vanish are the very recursion relations $\beta_n = \beta_n(\beta_1)$ for $n \geq 2$. For example, the recursion relation for $n = 2$

$$\beta_2 = \frac{1}{4} \beta_1^2 - 1.028 \beta_1 - 0.651 \quad (5)$$

is shown by the solid line in Fig. 1A.

For condensed-matter systems, the Dunham coefficients are related to the bulk modulus B by successive differentiation of Eq. 1 with respect to the interparticle distance R and substitution of the results into the expressions for the volume derivatives of Eq. 1. Hence,

$$\Delta = 9V_0 B_0 / (2E_0) \quad (6)$$

$$a_1 = 1 - B'_0 \quad (7)$$

$$a_2 = \frac{3}{4} \left[B_0 B''_0 + B'_0 (B'_0 - 1) + \frac{2}{9} \right] \quad (8)$$

where prime and subscript zero indicate differentiation with respect to pressure and equilibrium conditions (zero pressure), respectively (10). As accurate measurements of B''_0 are not available for the determination of $\beta_2 = a_2/\Delta$ for most solids, we propose the use of Eq. 5 to predict the fourth-order derivative of the binding energy, β_2 , for bulk cohesive systems. Our supposition is that the recursion relation derived from two-particle systems can be transferred to condensed matter. We can test this hypothesis by comparing Eq. 5 with β_1 and β_2 values derived from shock-wave experiments on solids. Indeed, when analyzed independently, these high-pressure data obey nearly the same β -correlation as diatomic molecules (10, 16).

The curve from Eq. 5, obtained from a fit to the diatomic-molecule data, reproduces experimental results for 38 solids quite well (Fig. 1B). In contrast, the Rydberg function with linear scaled distance z_1 [the Universal Binding Energy Relation of (17)] assumes that every β is constant, independent of the solids involved, which is incom-

patible with the data. For comparison with Eq. 5, the data for the 38 solids alone yield $h_1 = -0.906 \pm 0.024$ and $h_2 = 0.476 \pm 0.006$, which is similar to, though distinct from, the h_1 and h_2 values for the diatomic systems. Still, because the correlations for diatomic and condensed-matter systems differ little, we conclude that the vibrational properties of both have essential similarities in the statistical sense expressed by Fig. 1. The fact that we obtain coherent results is surprising: variations in chemical bonding and electronic states among the molecular and condensed-matter systems seem not to affect our correlations. The recursion relation (Eq. 5) appears to be transferable, as we supposed.

Three-parameter equations of state, including the Birch-Murnaghan (18) and Universal (19) forms, have been widely used to describe experimental compression data. Each of these forms involves the truncation of a series expansion, implicitly yielding a relation between a_1 and a_2 (20). The truncation relation for the Universal equation of state is compatible with many of the data (Fig. 1B), although it exhibits a slightly different curvature. For comparison, the Birch-Murnaghan relation is offset from the bulk of the data but is in better agreement with the results for the anharmonic solids toward the left of the figure (Li, Rb, and Na). Given the possibility of systematic biases in the data reduction [the assumptions given in (16)], we cannot argue that either one or the other of these forms is preferable.

Because of the truncations and the use of a linear U_s-u_p Hugoniot relation, each equation of state implies a specific relation

Fig. 1. (A) Correlation of the first two modified Dunham coefficients, β_1 and β_2 , determined from experimental data for 293 ground states (\bullet) and 46 excited states ($+$) of diatomic molecules [all cases for which the five parameters E_e , B_e , ω_e , α_e , and $\omega_e x_e$, which are necessary to evaluate Δ , β_1 , and β_2 , are presently available (15)]. Solid line is a plot of the β -curve (Eq. 5); large cross indicates the point predicted for a linear scaled distance z_1 . **(B)** Correlation of β_1 and β_2 determined from shock-wave data for 28 metals (\bullet) (38) and 10 compounds (\circ) (39), representing all the shock-wave measurements available for elements and simple compounds exhibiting no phase transitions or other features that complicate data reduction (16, 20, 21). Solid line is the $\beta_2(\beta_1)$ curve (Eq. 5) derived from diatomic systems; dashed line is a fit to the data for all of the 38 condensed-matter systems. The β values predicted by ($+$) the Universal Binding Energy Relation (17) and (\times) the Birch-Murnaghan (18) and (dotted line) Universal (19) equations of state are plotted for comparison.

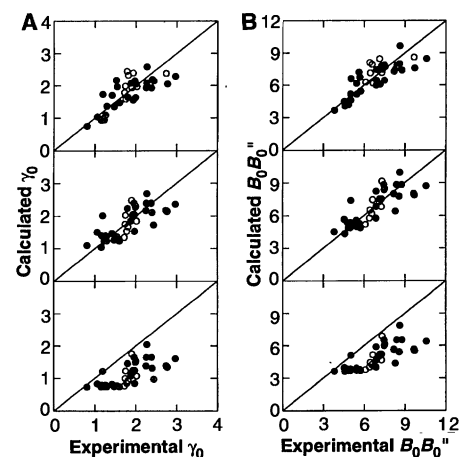
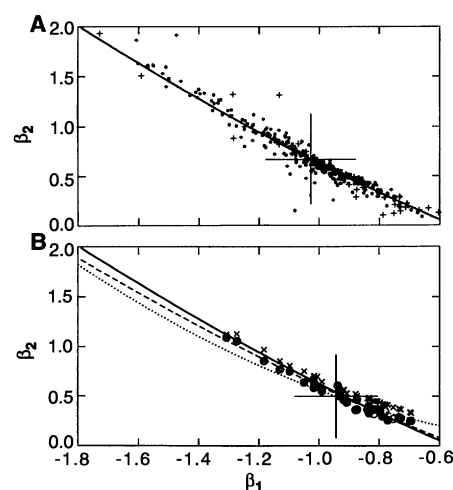


Fig. 2. Equilibrium thermodynamic variables **(A)** γ_0 and **(B)** $B_0 B''_0$ calculated from Eq. 5 (top) and from the Universal (middle) and Birch-Murnaghan (bottom) equations of state compared with experimental values. Symbols: (\bullet) and (\circ) as in Fig. 1; experimental γ_0 from (31, 32). Calculations based on a linear U_s-u_p relation with the Mie-Grüneisen form of equation of state.

between the zero-pressure values of B'_0 and both $B_0B'_0$ and the Grüneisen parameter γ_0 (16, 20, 21). The approach used here is at least as successful in reproducing the observed properties of our 38 test solids as the Birch-Murnaghan and Universal equations of state (Fig. 2). Correlations among the Dunham coefficients, a_1 and a_2 (Fig. 3), correspondingly show that for the solids we consider, the zero-pressure properties are generally well described by either the Universal or the present (Eq. 5) equations of state and by the Dugdale-MacDonald model for the Grüneisen parameter (20).

Each of the Universal and Birch-Murnaghan equations of state gives the equilibrium cohesive energy E_0 , as well as B'_0 , in terms of V_0 , B_0 , and B'_0 (Fig. 4) (20). Use of these calculated values for E_0 in Eq. 6, rather than the experimental values, yields an absolute comparison of β_1 and β_2 with the data, rather than just a comparison of trends (Fig. 1). In terms of the $\beta_2(\beta_1)$ curve, the Universal equation of state is now equivalent to the constant-value Universal Binding Energy Relation and does not reproduce the shock-wave measurements adequately (Fig. 4). The Birch-Murnaghan relation does define a trend comparable in slope to that of the data, but with a distinct offset from the measured values. Thus, a three-parameter equation of state or (equivalently) expression for the potential-energy curve does not describe the full range of observed data (Fig. 4). The present approach uses Eq. 5 and the experimental E_0 in a self-consistent manner to derive a four-parameter equation of state, and this

offers a more reliable description of the condensed-matter systems (Figs. 1 to 3).

Our analysis of equations of state, so far restricted to equilibrium (zero pressure) conditions, can be extended to address condensed matter at finite compression or expansion. We did this by calculating the internal energy change along the isentropes of the 38 test solids (22) and found that the curves of reduced cohesive binding energy for the 28 metals and 10 compounds are indistinguishable (within the uncertainties of the measurements and data reduction) when plotted against the nonlinear scaled distance z_2 obtained with the "diatomic value" $h_1 = -1.028$. Because we assumed that Eq. 5 and $h_2 = 0.670$ (again, the "diatomic value") are valid, z_3 is equivalent to z_2 for these solids (23), in accord with our hypothesis that the recursion relation obtained from diatomic systems can be transferred to condensed matter.

Even more remarkably, the reduced binding-energy curves for the 38 test solids closely overlap the Rydberg-Klein-Rees (RKR) potential-energy curves plotted against z_3 for 20 diatomic molecules (8). In fact, both molecular and condensed-matter curves are accurately represented by a Hulburt-Hirschfelder function, with $z = z_2$ for condensed matter and $z = z_3$ for diatomic molecules

$$F = [1 - \exp(-z)]^2 + cz^3 \exp(-az) - 1 \quad (9)$$

where $c = 1 + h_1$, $a = [(7/12) - h_2]/c$, $h_1 = -1.028$, and $h_2 = 0.670$ (8, 24). The first term on the right side of Eq. 9 is a Morse function, modified by the second term to yield the correct h values.

Finally, if we compare the reduced iso-

thermal pressure-volume relation obtained from Eq. 9 (25) with isothermal-compression measurements on a representative sampling of nine metallic elements [Cu, Ag, Mo, and Pd (26); Au (27); Pt (28); and Na, K, and Li (29)], we find that almost all of the experimental data fall on the Hulburt-Hirschfelder curve. This reinforces our conclusion, based on analysis of shock-wave data, that the correlations in energy parameters obtained from diatomic potentials can be transferred to condensed-matter systems.

Our work shows that a universal potential-energy function of the Hulburt-Hirschfelder form accurately represents the measured interactions for systems ranging from ground and excited states of diatomic molecules to condensed matter at high compression. Empirically, we find that the coefficients appearing in a series expansion of the potential energy are correlated and that the same correlation is found for diatomic and condensed-matter systems, within the uncertainties of the data. This finding has practical utility in that it allows us to formulate an improved equation of state for solids on the basis of the large number of measurements available from spectroscopy on diatomic molecules. Moreover, it suggests that there is an underlying similarity between the interatomic forces in condensed matter and diatomic systems that remains to be explained theoretically.

REFERENCES AND NOTES

1. G. C. Maitland, M. Rigby, E. B. Smith, W. A. Wakeham, *Intermolecular Forces, Their Origin and Determination* (Clarendon, Oxford, 1981).
2. J. N. Murrell, S. Carter, S. C. Farantos, P. Huxley, A. J. C. Varandas, *Molecular Potential Energy Functions* (Wiley, New York, 1984).
3. Y. P. Varshni, *Rev. Mod. Phys.* **29**, 664 (1957).
4. F. Jenč, *Adv. At. Mol. Phys.* **19**, 265 (1983).
5. J. Ferrante, J. R. Smith, J. H. Rose, *Phys. Rev. Lett.* **50**, 1385 (1983).
6. J. L. Graves and R. G. Parr, *Phys. Rev. A* **31**, 1 (1985).
7. J. Tellinghuisen, S. D. Henderson, D. Austin, K. P. Lawley, R. J. Donovan, *ibid.* **39**, 925 (1989).
8. K. S. Jhung, I. H. Kim, K.-H. Oh, K. B. Hahn, K. H. C. Jhung, *ibid.* **42**, 6497 (1990).
9. J. R. Smith, J. Ferrante, J. H. Rose, *Phys. Rev. B* **25**, 1419 (1982); J. Rose, J. P. Vary, J. R. Smith, *Phys. Rev. Lett.* **53**, 344 (1984).
10. K. S. Jhung, I. H. Kim, K.-H. Oh, K. H. C. Jhung, *Phys. Rev. B* **42**, 11580 (1990). The cohesive energy for crystals at equilibrium, E_0 , is obtained from the experimental heat of formation corrected for zero-point energy.
11. J. L. Dunham, *Phys. Rev.* **41**, 713 (1932); *ibid.*, p. 721.
12. $\Delta = \omega_e^2/(4B_e E_e)$, where ω_e is the harmonic frequency, B_e is the rotational frequency, and E_e is the sum of the dissociation and zero-point energies of the molecule.
13. The Morse and Rydberg functions with linear scaled distances (Eq. 2) are good examples of the latter case (6). These functions are determined by three parameters (including the Sutherland parameter) and have been successfully used to represent the potential-energy curves of various classes of diatomic molecules. It has been shown, however, that at least one more parameter is required to obtain a precise repre-

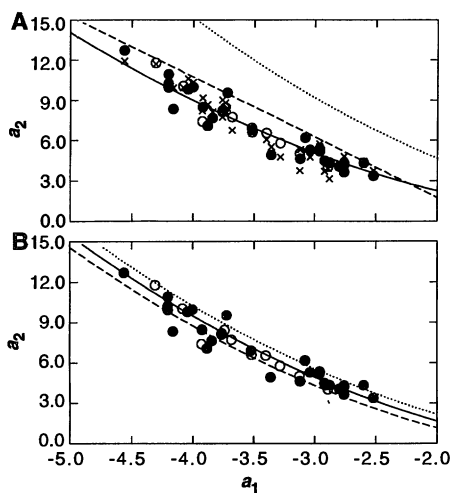


Fig. 3. Correlation of the Dunham coefficients, a_1 and a_2 , for condensed-matter systems. Experimental values [(●) and (○) as in Fig. 1] compared with various models of the (A) equation of state (×, Eq. 5; solid line, Universal; dashed line, Birch-Murnaghan; dotted line, Murnaghan) and (B) Grüneisen function (solid line, Dugdale-MacDonald; dashed line, Slater; dotted line, Vashchenko-Zubarev) (see 20).

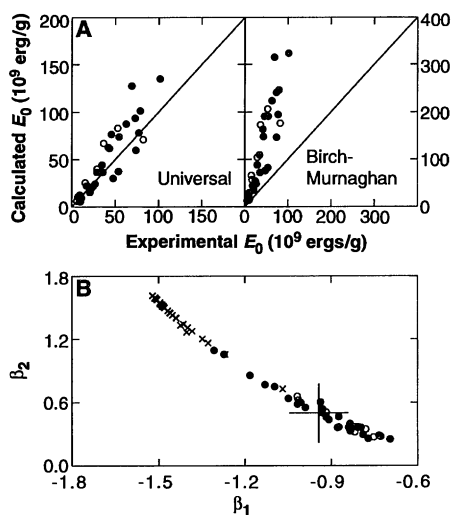


Fig. 4. (A) Calculated versus measured values of equilibrium cohesive energy and (B) the resultant absolute values of β obtained from the Universal (large cross) and Birch-Murnaghan (×) equations of state. (●) and (○) as in Fig. 1.

- sentation of the diatomic potential satisfying all of the available molecular data (6, 8, 30).
14. K. S. Jung, I. H. Kim, K.-H. Oh, K. H. C. Chung, *Phys. Rev. A* **44**, 4734 (1991).
 15. K. P. Huber and G. Herzberg, *Molecular Spectra and Molecular Structure* (Van Nostrand Reinhold, New York, 1979), vol. 4; see also the references in (8) and reference 9 in (14).
 16. In our analysis, we assume that the linear Hugoniot relation $U_s = C + Su_p$ holds, where U_s is the shock-wave velocity and u_p the particle velocity, and use the Mie-Grüneisen thermal correction, $\gamma/V = (\partial P/\partial E)_v$, where γ is the Grüneisen parameter [see (20, 21) for the data reduction and (31, 32) regarding γ].
 17. A. Banerjee and J. R. Smith, *Phys. Rev. B* **37**, 6632 (1988).
 18. F. Birch, *Phys. Rev.* **71**, 809 (1947); *J. Geophys. Res.* **83**, 1257 (1978).
 19. P. Vinet, J. Ferrante, J. R. Smith, J. H. Rose, *J. Phys. C* **19**, L467 (1986).
 20. R. Jeanloz, *J. Geophys. Res.* **94**, 5873 (1989). One can obtain cohesive energies from the equations of state by taking the limit $V \rightarrow \infty$ [the corresponding finite-strain parameter (18) $f \rightarrow -1/2$]; that is, we extrapolate the condensed-matter equations of state to infer the energy at infinite expansion. Note that the Universal equation of state yields more satisfactory values for the cohesive energy than does the Birch-Murnaghan equation of state (Fig. 4).
 21. A. L. Ruoff, *J. Appl. Phys.* **38**, 4976 (1967).
 22. The analysis involves reduction of the shock-wave data by the same approach described above (10, 20), along with the assumption that γ/V is constant [see (33) for data reduction]. The reason we calculated the energy change along the isentrope was that this minimizes the assumptions involved in the thermal correction from the Hugoniot state. Of course, if we had used zero-temperature values for the material variables, we would have obtained the conventional cohesive binding-energy relation as a function of distance. In our analysis, we also restricted the volume (or interparticle distance) to less than that at the ideal critical point, that is, the minimum point of the reduced isentrope, where the bulk sound speed goes to zero. At this point, the material no longer transmits sound waves, which implies that the ideal tensile strength has been exceeded (34).
 23. Use Eq. 5 to cancel the second term on the right side of Eq. 4.
 24. H. M. Hulburt and J. O. Hirschfelder, *J. Chem. Phys.* **9**, 61 (1941).
 25. The pressure-volume (P - V) relation, expressed in reduced form, is

$$P_R = P/(E_0 \partial z/\partial V) = -dF/dz = 2 \exp(-z) [\exp(-z) - 1] + c (az - 3)z^2 \exp(-az)$$
 with terms defined in Eq. 9. In analyzing the data, we made thermal corrections to Δ and β_1 through E_0 , B_0 , and B_0' (35): we considered both the lattice vibrational and electronic contributions to the thermal energy, the first being approximated by a Debye model (36, 37).
 26. H. K. Mao, P. M. Bell, J. W. Shaner, D. J. Steinberg, *J. Appl. Phys.* **49**, 3276 (1978).
 27. D. L. Heinz and R. Jeanloz, *ibid.* **55**, 885 (1984).
 28. J. A. Morgan, *High Temp. High Pressures* **6**, 195 (1974).
 29. M. S. Anderson and C. A. Swenson, *Phys. Rev. B* **28**, 5395 (1983); *ibid.* **31**, 668 (1985).
 30. J. Ferrante, H. Schlosser, J. R. Smith, *Phys. Rev. A* **43**, 3487 (1991).
 31. *Los Alamos Scientific Laboratory Report LA-4167-MS* (Los Alamos, NM, 1969).
 32. S. N. Vaidya and G. C. Kennedy, *J. Phys. Chem. Solids* **32**, 951 (1971).
 33. F. E. Prieto and C. Renero, *ibid.* **37**, 151 (1976); E. S. Lee, S. S. Lee, K. S. Jung, I. H. Kim, *Korean J. Appl. Phys.* **2**, 121 (1989).
 34. R. G. McQueen and S. P. Marsh, *J. Appl. Phys.* **33**, 654 (1962).
 35. J. Berger and S. Joigneau, *C. R. Acad. Sci. Paris* **249**, 2506 (1959).
 36. V. N. Zharkov and V. A. Kalinin, *Equations of State*

- for Solids at High Pressures and Temperatures* (Consultants Bureau, New York, 1971).
37. L. V. Al'tshuler, S. B. Korner, A. A. Bakanova, R. F. Trunin, *Sov. Phys. JETP* **11**, 573 (1960).
 38. S. P. Marsh, Ed., *LASL Shock Hugoniot Data* (Univ. of California Press, Berkeley, 1980).

39. H. C. Rodean, *J. Chem. Phys.* **49**, 4117 (1968).
40. This work was supported by the National Aeronautics and Space Administration and the National Science Foundation.

3 September 1992; accepted 18 February 1993

Rates of Electron Emission from Negatively Charged, Impact-Heated Fullerenes

Chahan Yeretizian, Klavs Hansen, Robert L. Whetten

Thermal emission of electrons is ordinarily considered to be exclusively a property of macroscopic condensed matter. Slow electron emission occurs for certain small metal clusters as well as for silicon and carbon clusters, but the nature of this process has not been established. Electron emission rates have been obtained and analyzed from extensive real-time measurements on negatively charged fullerenes for several sizes and over a wide, continuous range of energies. These results confirm that delayed electron emission is a simple activated process that depends strongly on the internal energy and size of the cluster and that it has a common underlying mechanism, independent of size. However, the Arrhenius form deduced is inconsistent with the emission rate theory used for bulk surfaces. These results allow the question of the correct microscopic description of this newly observed electron emission process to be assessed.

Electron emission from an excited atom or molecule is considered a prompt process, occurring on an electronic time scale (10^{-16} s), except where particular autoionizing resonances are involved (1). On the other hand, condensed matter—for example, a tungsten filament—may exhibit thermal emission, characterized by activated rates that increase smoothly with excitation energy or temperature; the statistical rate theory of thermionic emission gives a successful microscopic description of this process (2). Several recent reports have documented observations of slow electron emission from strongly bound atomic clusters including tungsten (3), carbon (4, 5), and silicon (6); this discovery is considered promising in terms of attempts to develop a thermometry of clusters and is thought to reflect the emergence of bulk-like electronic structure. The recent examples of slow electron emission from large molecules and clusters are suggestive of a nonprompt emission mechanism, similar to emission from conducting surfaces. When strongly excited, by subthreshold radiation or by surface impact or atom bombardment, the neutral clusters of these elements cool through emission of an electron, either in competition with fragmentation or in its place. In an extreme case, irradiation of giant positively charged fullerenes, C_n^+ ($n > 200$), suspended in a magnetic trap, generates doubly charged molecules (C_n^{2+}), evidently by slow electron emission (7).

In the case of negatively charged clusters

and negative molecular ions, it is less unusual that electrons are emitted preferentially to fragmentation, given that electron affinities often lie well below the fragmentation thresholds (8). Smalley and co-workers (9), in attempted photoelectron spectrum measurements, found that hot or multiphoton-excited C_{60}^- gives very broad time-of-flight (TOF) profiles limited only by the ion transit through the instrument. At the same time, it was reported that the electron emission peak arising from surface scattering of C_{60}^- (10), small carbon (C_n^-), or small silicon (Si_n^-) clusters (6) is strongly broadened at the threshold impact energy for electron ejection.

These reports raise unresolved questions regarding the nature of delayed emission in larger negatively charged atomic clusters, including whether a single rate can be defined and whether the process is thermally activated and describable by rate expressions already put forward. In particular, one would like to know how the rate depends on the cluster energy content and on the characteristics of the system, including electron affinity, size, and the spectrum of electronic excited states as well as the electron-ion coupling. Since the early days of activated rate theory, the precise measurement of the preexponential factor and the temperature dependence of the rate constant of specific unimolecular reactions have revealed the key information needed to deduce the underlying mechanism. The goal of our work has been to provide the necessary experimental information and to stimulate the development of appropriate physical models.

Department of Chemistry and Biochemistry, University of California, Los Angeles, CA 90024-1569.